Anthocyanin–aluminium and –gallium complexes in aqueous solution

M. Elhabiri,[a] **P. Figueiredo,**[a] **K. Toki,**[b] **N, Saito**[c] **and R. Brouillard** *,[a]

[a] *Laboratoire de Chimie des Polyphénols, associé au CNRS, Université Louis Pasteur, Faculté de Chimie, 1, rue Blaise Pascal 67008 Strasbourg Cedex, France*
[b] *Laboratory of Floriculture, Minami-Kyushu University, Takanabe, Miyazaki, Japan*
[c] *Chemical Laboratory, Meiji-Gakuin University, Totsuka-ku, Yokohama, Japan*

Complexation of aluminium and gallium ions with synthetic anthocyanin models and natural anthocyanins extracted from the blue flowers of *Evolvulus pilosus* cv 'Blue Daze' and the violet flowers of *Matthiola incana* has been thoroughly investigated in aqueous solution. From UV–VIS spectroscopic data collected at pH 2–5, the presence of complexes, involving not only the coloured forms but also the colourless forms of the pigments is demonstrated. A theoretical treatment is developed for the calculation of the corresponding stability constants. The pigments studied throughout this work can be divided into two series, one sharing a cyanidin chromophore and the other a delphinidin one. Within both series, individual pigments are distinguished according to the degree and type of glycosylation and/or acylation. Intramolecular effects such as copigmentation of anthocyanin–aluminium complexes and the effect of the presence of a malonyl group on the formation of those complexes are discussed. These results are important to plant pigmentation and, for instance, a narrow pH domain in which colour amplification due to complexation is at a maximum has been found.

Introduction

The chromophore units of anthocyanins are hydroxy- and methoxy-derivatives of the 2-phenylbenzopyrylium (flavylium) structure. They occur as non-plastid, water soluble glycosylated pigments dissolved in the vacuolar cell sap, predominantly in the epithelial tissue of flowers and fruits, more rarely in stems and leaves.[1,2] These hydroxy- and methoxy-flavylium derivatives exist as glycosides of hydroxy groups (mainly at the 3 and 5 positions) of the benzopyrylium core. The glycosylating sugars may be mono-, di- or tri-saccharides, and the aglycone forms are known as anthocyanidins (Scheme 1). Additionally, anthocyanins may be acylated through esterification of the sugar residues with one or more of a variety of aliphatic acids, phenolic benzoic acids or phenolic cinnamic acids.

$R^5 = H, \beta\text{-D-Glycosyl}$
$R^{3'} = R^{5'} = H, OH, OCH_3$
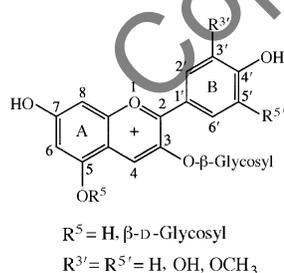
Scheme 1 The flavylium form of common natural anthocyanins

The more common anthocyanins (3-monoglucosides and 3,5-diglucosides), rapidly fade when put in mildly acidic aqueous solutions. Indeed, the water molecule readily reacts at position 2 of the flavylium cation with the consequent formation of large amounts of colourless forms (hemiacetal and chalcones) according to a reversible process called the hydration reaction (Scheme 2). *In vivo*, these pigments may be found in association with metal ions, other flavonoids (which may themselves be glycosylated and acylated) and probably with polysaccharide macromolecular carriers. All these interactions affect the absorption spectra of the anthocyanins involved and thus they give access to the mechanisms explaining the great variations in plant colours. It is now well known that colourless polyphenols (flavones, flavonols, cinnamic and benzoic acid esters, tannins) are able to form molecular, non-covalent, stacking complexes with the large planar, π-electron rich flavylium nucleus. We have demonstrated that the hydrophobic interaction efficiently protects the chromophore against nucleophilic attack from water, displacing at the same time the overall equilibrium between the coloured and colourless forms towards the selectively complexed coloured forms.[3–7] This phenomenon, called copigmentation, can also operate in an intramolecular way in more complex anthocyanins bearing cinnamic or benzoic acid residues on their glycosyl groups, leading to stable coloured solutions at mildly acidic pH values.[2,8,9,17]

Unlike polyphenolic copigments, metal ions which could be present in the anthocyanin natural media seem more rarely involved in colour stabilization. However, small highly charged metal ions such as Al^{3+} and Mg^{2+} have been reported possibly to strengthen the pigment–copigment interaction leading to hyperchromic and bathochromic shifts. In particular, it has been proposed that the blue colour displayed by some flowers is the result of pigment–copigment–metal ion assemblies.[3,21,22] The most remarkable achievement in that field is the X-ray structure of the commelinin pigment elucidated by Goto and Kondo, which shows up to six pigment and six copigment molecules packed around two magnesium ions in a crystalline state.[2]

A first report[10] on anthocyanin–aluminium complexation has provided information on the mechanism of complexation. From UV–VIS spectroscopic measurements on equilibrated solutions at different pH values and relaxation kinetics measurements (pH-jump), the binding constants have been calculated and the percentage of different free and complexed pigment forms plotted as a function of pH. ^{1}H NMR analysis in CD_3OD (in which complexation is much stronger than in water), has confirmed the conversion of the anthocyanin from the red flavylium form to the deep-purple quinonoidal forms upon coordination to Al^{3+}.
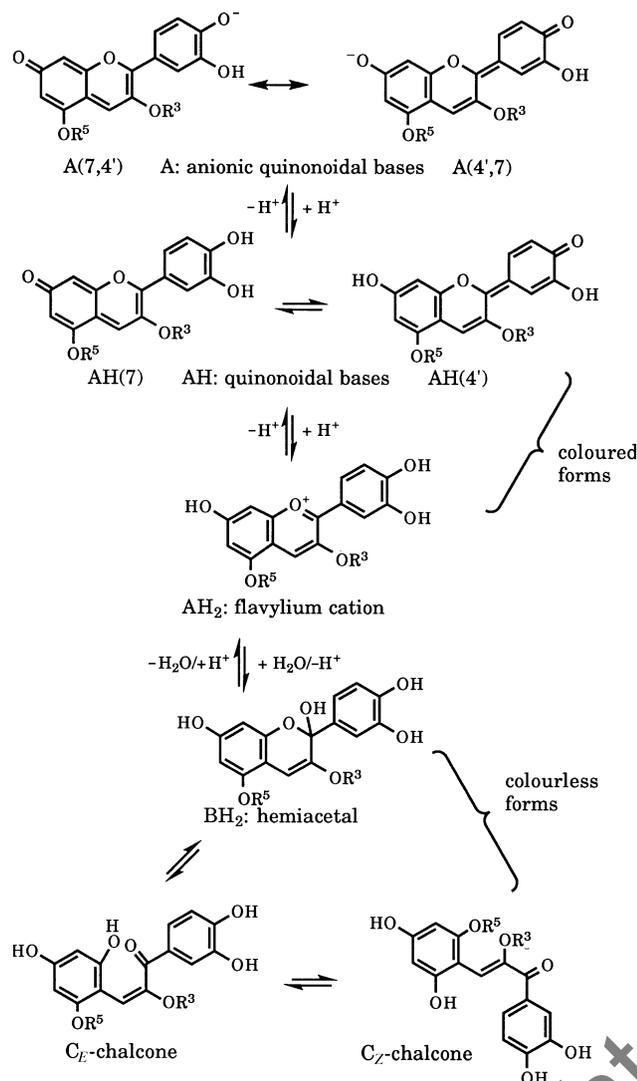
Scheme 2 The structural transformations of anthocyanins in slightly acidic to neutral solutions

Scheme 3 Structures of the extracted anthocyanins

4: $R^3 = R^5 = O\text{-}\beta\text{-}D\text{-glucosyl}$, $R^7 = H$
5: $R^3 = O\text{-}\beta\text{-}D\text{-}[6\text{-}O\text{-}(6\text{-deoxy})\text{-}\alpha\text{-}L\text{-mannosyl}]$-
  glucosyl, $R^5 = OH$, $R^7 = H$
A1: $R^3 = OCH_3$, $R^5 = R^7 = H$
A2: $R^3 = OCH_3$, $R^5 = H$, $R^7 = CH_3$
A3: $R^3 = R^5 = R^7 = H$
A4: $R^3 = R^5 = H$, $R^7 = CH_3$
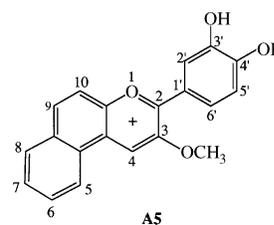
Scheme 4 Structures of the natural anthocyanins **4** and **5** and the synthetic artificial flavylium chlorides **A1** to **A5**

In this work, spectroscopic measurements on aluminium– and gallium–anthocyanin systems are interpreted according to a theoretical treatment so as to give information on the stability and relative abundance of metal complexes as a function of pH, and also on the mechanisms leading to their formation. Influence of malonyl and acyl groups, born by the glycosyl groups, on metal complexes production and stabilization is also discussed by comparing two series of acylated anthocyanins with either a cyanidin or a delphinidin aglycone, respectively extracted from the violet flowers of *Matthiola incana*[11] and the blue flowers of *Evolvulus pilosus* cv 'Blue Daze'.[12] Their structures (Scheme 3), fully elucidated by ^{1}H NMR and FAB-MS techniques, are 3-*O*-(2-*O*-β-D-xylopyranosyl-β-D-gluco-pyranosyl)-5-*O*-β-D-glucopyranosyl cyanidin **1**, 3-*O*-{6-*O*-(*trans*-caffeyl)-2-*O*-[2-*O*-(*trans*-synapyl)-β-D-xylopyranosyl]-β-D-glucopyranosyl}-5-*O*-[6-*O*-(malonyl)-β-D-glucopyranosyl]-cyanidin **2**, 3-*O*-{6-*O*-(*trans*-feruyl)-2-*O*-[2-*O*-(*trans*-synapyl)-β-D-xylopyranosyl]-*O*-β-D-glucopyranosyl}-5-*O*-[6-*O*-(mal-onyl)-*O*-β-D-glucopyranosyl]cyanidin **3**, 3-*O*-[6-*O*-(*trans*-4-*O*-{6-*O*-[*trans*-3-*O*-(*O*-β-D-glucopyranosyl)-caffeyl]-*O*-β-D-gluco-pyranosyl}-caffeyl)-β-D-glucopyranosyl]-5-*O*-[(6-*O*-malonyl)-β-D-glucopyranosyl]delphinidin **B**, 3-*O*-[6-*O*-(*trans*-caffeyl)-*O*-β-D-glucopyranosyl)-5-*O*-[(6-*O*-malonyl)-β-*O*-D-glucopyrano-syl]delphinidin **B1** and 3-*O*-β-D-glucopyranosyldelphinidin **B2** (Scheme 3). 3,5-Di-*O*-β-D-Glucopyranosylcyanidin chloride (also known as cyanin chloride) **4**, 3-*O*-[6-*O*-(6-deoxy)-α-L-

mannosyl]-β-D-glucopyranosylcyanidin chloride (also known as antirrhinin chloride) **5**, 3',4',7-trihydroxy-3-methoxy-flavylium chloride **A1**, 3',4'-dihydroxy-3,7-dimethoxyflavylium chloride **A2**, 3',4',7-trihydroxyflavylium chloride **A3**, 3',4'-dihydroxy-7-methoxyflavylium chloride **A4** and 2-[(3',4'-di-hydroxy)phenyl]-3-*O*-methyl-naphtho[2,1-*b*]pyrylium chloride **A5** were also studied for comparison (Scheme 4).

Experimental

Materials

The 3-*O*-β-D-glucopyranosyldelphinidin **B2** and cyanin chloride **4** were a kind gift from Professor Samuel Asen and were used without further purification. Compounds **5**, **A1**, **A3** and **A5** were synthesized and purified according to procedures described elsewhere.[13–15] All the other acylated pigments (Scheme 3) studied were isolated according to published procedures.[11,12] Aluminium chloride hexahydrate (99% pure) was purchased from Aldrich and anhydrous gallium chloride from Strem, and were used as supplied.

The flavylium chloride **A2** was synthesized according to Scheme 5. Reduction of 2′-chloro-3,4-dihydroxyacetophenone by zinc powder in acetic acid–tetrahydrofuran mixture led to 3,4-dihydroxyacetophenone. The corresponding enol ether was prepared in high yield (88%) *via* the *in situ* formation of trimethylsilyl iodide.[15] Methoxylation of the trimethylsilyl enol ether of 3,4-trimethylsilyloxyacetophenone was adapted from a procedure developed by Moriarty and co-workers,[16] commercially available iodosobenzene diacetate replacing iodosobenzene. The yield was *ca.* 40% after chromatography on silica gel. In the final condensation step, gaseous hydrogen chloride was gently bubbled (3 h) into an equimolar solution of 2′-methoxy-3,4-dihydroxyacetophenone and 2-hydroxy-4-methoxybenzaldehyde in distilled ethyl acetate at *ca.* 0 °C. Red crystals of 3′,4′-dihydroxy-3,7-dimethoxyflavylium chloride were formed and the reaction was completed by keeping the mixture at −20 °C for 3 d. The crystals were filtered off, thoroughly washed with ethyl acetate and dried under vacuum (yield: 65%). Compound **A2** was characterized by electrospray mass spectrometer (positive mode, *m/z* = 298.73), UV–VIS spectroscopy (λ_{max} 276 and 498 nm in 0.1 mol dm^{-3} HCl) and ^{1}H NMR δ_H [200 MHz, $(CD_3)_2SO$–CF_3CO_2D; *J* in Hz]: 8.75 (s, H-4), 8.14 (dd, *J* 8.7 and 2.2, H-6′), 8.10 (d, *J* 2.2, H-2′), 7.94 (d, *J* 9, H-5), 7.54 (d, *J* 2.2, H-8), 7.30 (dd, *J* 9 and 2.2, H-6), 6.98 (d, *J* 8.6, H-5′), 4.08 (s, CH_3), 3.96 (s, CH_3).

3′,4′-Dihydroxy-7-methoxyflavylium chloride **A4** was obtained by condensation under acidic conditions (gaseous hydrogen chloride–ethyl acetate) of 3,4-dihydroxyacetophenone and 2-hydroxy-4-methoxybenzaldehyde, and characterized by electrospray MS (positive mode, *m/z* 268), UV–VIS spectroscopy (λ_{max} 275 and 498 nm in 0.1 mol dm^{-3} HCl) and ^{1}H NMR δ_H [400 MHz, $(CD_3)_2SO$–CF_3CO_2D]: 9.17 (d, *J* 9, H-4), 8.48 (d, *J* 9, H-3), 7.50 (dd, *J* 9 and 2.4, H-6′), 7.87 (d, *J* 2.2, H-2′), 8.20 (d, *J* 9, H-5), 7.94 (d, *J* 2.3, H-8), 8.06 (dd, *J* 8.7 and 2.4, H-6), 7.11 (d, *J* 8.6, H-5′), 4.06 (s, CH_3).

The purity of **A2** and **A4** was checked by reverse-phase HPLC on a Merck C-8 column (5 μm, 125 mm × 4 mm) with a flow rate of 1 ml min^{-1} and a linear gradient elution for 30 min from 5–20% solvent A [5% HCO_2H in CH_3CN–H_2O (1:1)] in solvent B (5% HCO_2H in H_2O) followed by a linear gradient elution for 30 min from 20% solvent A in solvent B to 100% solvent A. Chromatograms were recorded with a Spectra-Physics apparatus equipped with a Hewlett Packard diode-array detector monitoring at 260 and 500 nm.

Absorption spectra

Absorption spectra were recorded with a Hewlett Packard diode-array spectrophotometer fitted with a quartz cell (*d* = 1 cm) equipped with a stirring magnet. A constant temperature of 25 ± 0.1 °C, measured with a Comark thermocouple, was maintained in the spectrometer cell by use of a Lauda water-thermostatted bath. Water used in samples preparation was distilled, deionized and ultrafiltered to a resistance of *ca.* 18 MΩ using a Millipore Milli-Q apparatus. Methanol was spectroscopy grade (Merck).

pH Measurements

The pH of the solutions was recorded with a Metrohm model
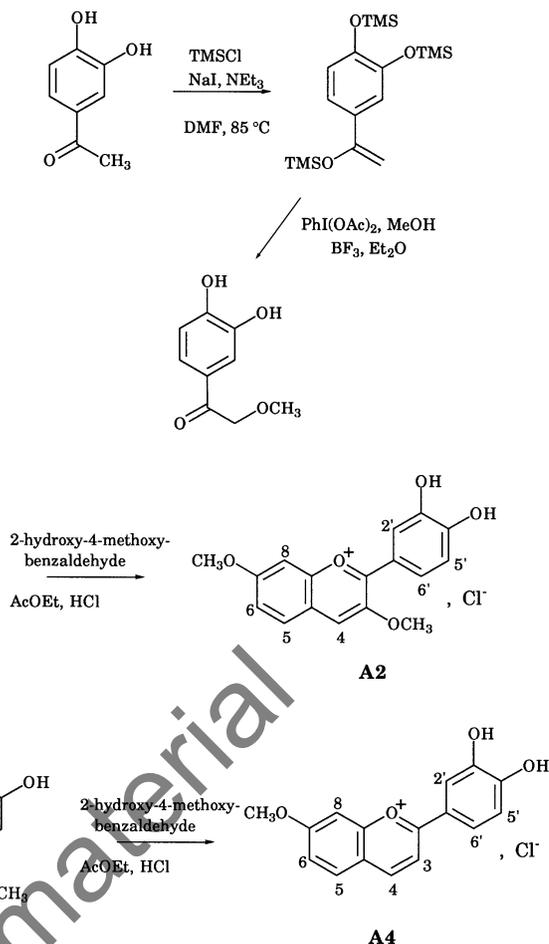
Scheme 5 Synthesis of 3′,4′-dihydroxy-3,7-dimethoxyflavylium chloride **A2** and 3′,4′-dihydroxy-7-methoxyflavylium chloride **A4**

654 pH meter fitted with a small combined glass electrode. The buffers used for calibration were pH 7 and pH 4 Aldrich standards.

Data analysis

The curve fittings were carried out on a Macintosh IIsi computer using the KALEIDAGRAPH program. Standard deviations are reported.

Semi-empirical quantum mechanical calculations

Semi-empirical quantum mechanical calculations were performed on an Escom Pentium P100 PC using the HYPER-CHEM program (version 4, Hypercube, Inc., Ont., Canada) in the MM$^+$ and AM1 parametrizations.

Thermodynamic measurements

Structural transformations (general procedure). Mother solutions of *ca.* 10^{-5}–10^{-4} mol dm^{-3} of all the anthocyanins were prepared in 0.1 mol dm^{-3} HCl and left to equilibrate in the dark for 2 h. Then, for each pigment 10 solutions were prepared by 1:10 dilutions of the mother solutions with increasing volumes of NaOH (0.1 mol dm^{-3}) so that the final pH covered was 1.0–5.0. The value of the thermodynamic constant K'_h of the overall hydration equilibrium connecting the flavylium ion AH_2 and the mixture of colourless forms, hemiacetal BH_2 and chalcone forms, was gained from recording the visible absorbance at the maximum visible wavelength of flavylium absorption (*D*) on fully equilibrated solutions at different pH values [eqn. (1); see later, D_0 being the visible absorbance at the

$$\frac{D_0}{D_0 - D} = \frac{K'_h + K_a + 10^{-pH}}{K'_h + K_a(1 - \varepsilon_{AH_2}/\varepsilon_{AH})} \qquad (1)$$

Table 1 Thermodynamic, kinetic and spectroscopic constants of the structural transformations of the flavylium cations in aqueous solution at 25 °C (see text for definitions)

Compound	pK'_h	pK_a	K_1	k_1/min^{-1}	$k_2/mol^{-1} dm^3 min^{-1}$	$\varepsilon_{AH_2}/mol^{-1} dm^3 cm^{-1}$	$\lambda_{max}(AH_2)/nm$
1[a]	1.29 ± 0.02	4.57 ± 0.06		$(4.93 \pm 0.06)10^2$	$(0.95 \pm 0.06)10^4$	3 600	522
2[b]	1.78 ± 0.01	2.26 ± 0.01	8.70	$(38.52 \pm 0.27)10^2$	$(21.41 \pm 0.15)10^4$	21 200	536
3[b]	2.75 ± 0.02	2.01 ± 0.02	8.20	$(3.49 \pm 0.03)10^2$	$(19.42 \pm 0.16)10^4$	15 100	538
4[a]	2.07 ± 0.02	4.03 ± 0.02		$(2.92 \pm 0.03)10^2$	$(3.45 \pm 0.03)10^4$	35 000	510
5[a]	2.93 ± 0.02	3.58 ± 0.03		$(1.01 \pm 0.01)10^2$	$(8.68 \pm 0.07)10^4$	7 000	500
B[c]	3.23 ± 0.06	4.46 ± 0.04		36.5 ± 0.3	$(6.20 \pm 0.06)10^4$	32 400	538
B1[c]	2.30 ± 0.02	4.52 ± 0.05		96.5 ± 0.8	$(1.93 \pm 0.04)10^4$	23 400	526
B2[c]	2.36 ± 0.05	3.62 ± 0.07		6.9 ± 0.1	$(1.58 \pm 0.01)10^3$	23 400	516
A1[d]	2.42 ± 0.02	4.40 ± 0.06		23.2 ± 1.5	$(6.1 \pm 0.4)10^3$	27 400	500
A2[d]	2.03 ± 0.03	4.16 ± 0.07		$(4.21 \pm 0.05)10^{-2}$	4.93 ± 0.06	33 130	494
A3[d]	2.91 ± 0.03	4.35 ± 0.04		e	e	28 500	480
A4[d]	2.90 ± 0.02	4.85 ± 0.05		e	$(3.82 \pm 0.06)10^3$	30 050	470
A5[d]	3.05 ± 0.04	4.19 ± 0.05		$(5.56 \pm 0.02)10^3$	$(6.24 \pm 0.06)10^6$	31 650	516

[a] Ref. 18. [b] In these cases, pK'_h and pK_a must be considered as pK_h^{CP} and pK_a^{CP} (see ref. 18). [c] Ref. 9(c). [d] This work. [e] Not determined.

visible maximum wavelength of flavylium absorption for an equilibrated solution at pH less than 1]. The value of the constant K_a of the AH_2/AH proton-transfer equilibrium was obtained from pH-jump experiments and curve fitting of the plot of the apparent rate constant of hydration (first-order) vs. final pH [eqn. (2)]. Both procedures have been recently published with full details.[9,10]

$$\frac{K'_h + K_a + 10^{-pH}}{k} = \frac{1}{k_2} + \frac{K_a}{k_2 \times 10^{-pH}} \qquad (2)$$

Complexation equilibria. Mother solutions of ca. 10^{-5}–10^{-4} mol dm^{-3} of all anthocyanins were prepared in 0.1 mol dm^{-3} HCl (and 2–3% MeOH for anthocyanins of low solubility) and left to equilibrate in the dark for 2 h. A 0.1 mol dm^{-3} solution of $AlCl_3 \cdot 6H_2O$ was prepared in a 3.8 pH buffer. A range of solutions of pH 2.0–5.0 in CH_3CO_2H–CH_3CO_2Na buffers were prepared in the following way. 1 ml of a mother solution and 1 ml of the metal ion solution were mixed and diluted with different pH buffers so that the final volume was 10 ml and the final pH 2.0–5.0. The final solutions were allowed to equilibrate in the dark for ca. 3 h. Values of the complexation constants were gained from a curve fitting of the visible absorbance (at a given wavelength) vs. pH plot according to eqns. (3) and (4) (see later).

Kinetic measurements
A 1 ml sample of each equilibrated aqueous solution of anthocyanin, at different pH (1.0–2.5) was magnetically stirred in the spectrophotometer cell. To these solutions 1 ml of phosphate buffer solutions, ranging in pH from 4.3 to 7.4, was quickly added (mixing time of the order of 1 s), and the visible absorption maximum was recorded every second, over 120 s, to full completion of the hydration equilibrium. The final pH was then measured and shown to range from 2.3 to 5.0. The spectrometer software automatically computes the hydration first-order apparent rate constant, as well as the absorbance once the equilibrium state at the new pH value is finally attained. The standard deviations were less than 2%. In the calculations, the concentration of the hydronium ion is approximated to 10^{-pH}. The theoretical treatment that ensues for the obtention of the rate constants is given in full detail in ref. 9.

Results

Anthocyanins having a catechol or a pyrogallol group in their structure are widespread in flowers. They usually appear as glycosylated derivatives of the cyanidin, delphinidin and petunidin chromophores. Reaction of metal ions like iron(III) and aluminium(III) with such flavylium systems has been used for a long time as a qualitative test showing the presence of a catechol group in plant anthocyanins. The test is based on

the observation of a colour change, or a bathochromic shift of the visible λ_{max}, on addition of aluminium ion, usually as $AlCl_3$.[17] Moreover, aluminium being relatively abundant in plants, its complexation with anthocyanins could be of biological relevance in the expression of the blue colour in flowers.

Anthocyanins structural transformations (exception is made for compounds 2 and 3)
The combination of thermodynamic and kinetic measurements allows us to estimate the values for the following parameters: the thermodynamic constant of the AH_2/AH proton transfer reactions K_a, the thermodynamic constant of the overall hydration of AH_2 into the mixture of colourless hemiacetal and chalcone forms K'_h, the rate constants of the hydration process (k_1 and k_2 for the forward and backward reactions, respectively) connecting AH_2 with the hemiacetal BH_2 which in our kinetic experiments is indistinguishable from the E-chalcone C_E because of the very fast ring–chain tautomerism. The corresponding thermodynamic constant is denoted K_h and equals k_1/k_2. K'_h, K_a are defined as a_H ($[BH_2] + [C_E] + [C_Z]$)/$[AH_2]$, a_H $[AH]/[AH_2]$, respectively, a_H being 10^{-pH}. K_h is thus expressed as a_H ($[BH_2] + [C_E]$)/$[AH_2]$. The thermodynamic constant of the Z–E isomerism (K_i) can be estimated from the relationship, $K'_h = K_h(1 + K_i)$ (Scheme 6). Values of K'_h, K_a, k_1 and k_2 are reported in Table 1.

$$AH_2 + H_2O \rightleftharpoons BH_2 + C_E + C_Z + H^+$$
$$AH_2 \rightleftharpoons AH + H^+$$
$$C_E \rightleftharpoons C_Z$$
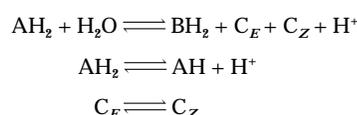
Scheme 6

Structural transformations of compounds 2 and 3 (special cases)
For this kind of acylated pigments, it has been shown that at pH > 1, intramolecular copigmentation occurs giving rise, for the flavylium cation, to a special conformation CP with a smaller ε value than that of the flavylium ion at pH < 1.[18] In these two particular cases, K'_h and K_a are denoted K_h^{CP} and K_a^{CP} and redefined as a_H ($[BH_2] + [C_E] + [C_Z]$)/$[CP]$ and $a_H[AH]/[CP]$, and K_1, the equilibrium constant of the flavylium cation conformational change, is given by $[CP]/[AH_2]$ (Table 1). The theoretical treatment that follows for the obtention of the equilibrium rate constants is described in ref. 17 [see eqn. (10) and Fig. 3 in the reference].

Complexation equilibria
The experimental curves of Fig. 1 are best fitted by theoretical curves postulating formation of two metal complexes of 1:1 stoichiometry, one (AM) involving the coloured forms of the pigment and the other (BM) involving the colourless forms taken as a whole (Scheme 7). When complex formation is

Table 2 Thermodynamic constants of complexation of the flavylium cations with Al^{3+} and Ga^{3+} in acetate buffers at 25 °C (see text for definitions)

| Compound | Al^{3+} | | Ga^{3+} | | |
	pK_{AM}	pK_{BM}	pK_{AM} [a]	pK_{BM} [a]	$\lambda_{max}(AM)/nm$
1	2.96 ± 0.04	b			590
2	2.66 ± 0.04	b			580
3	2.84 ± 0.05	b			580
4	3.13 ± 0.03	4.84 ± 0.06			556
5	4.05 ± 0.05	5.22 ± 0.04			555
B	2.59 ± 0.08	5.67 ± 0.04	2.24 ± 0.05		584
B1	2.33 ± 0.06	7.05 ± 0.04			582
B2	3.53 ± 0.04	6.64 ± 0.08			568
A1	4.04 ± 0.06	6.39 ± 0.05	3.56 ± 0.09	6.06 ± 0.08	544
A2	3.17 ± 0.04	5.81 ± 0.06	3.29 ± 0.05	8.15 ± 0.05	548
A3	4.36 ± 0.02	6.17 ± 0.04	2.26 ± 0.07	4.23 ± 0.09	526
A4	4.12 ± 0.09	6.82 ± 0.12	2.24 ± 0.08	4.64 ± 0.08	528
A5	4.25 ± 0.12	5.84 ± 0.16			566

[a] In the case of gallium many pK_{AM} and pK_{BM} values are not available due to very limited amounts of the corresponding pigments. [b] BM not detected.
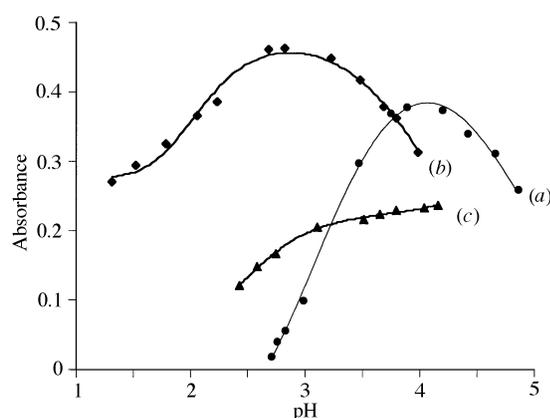
Fig. 1 (*a*) Plot of absorbance (548 nm) *vs*. pH for equilibrated solutions of 3′,4′-dihydroxy-3,7-dimethoxyflavylium chloride **A2** and Al^{3+} in 0.5 mol dm^{-3} acetate buffers (T 25 °C). Pigment concentration: 5.25×10^{-5} mol dm^{-3}. Al^{3+}: pigment molar ratio: 190 : 1. The solid line is the result of the curve fitting according to eqn. (4) ($r = 0.998$). (*b*) Plot of absorbance (548 nm) *vs*. pH for equilibrated solutions of 3′,4′-dihydroxy-3,7-dimethoxyflavylium chloride **A2** and Ga^{3+} in 0.5 mol dm^{-3} acetate buffers (T 25 °C). Pigment concentration: 3.0×10^{-5} mol dm^{-3}. Ga^{3+}: pigment molar ratio: 167 : 1. The solid line is the result of the curve fitting according to eqn. (4) ($r = 0.994$). (*c*) Plot of absorbance (580 nm) *vs*. pH for equilibrated solutions of anthocyanin **3** and Al^{3+} in 0.5 mol dm^{-3} formate buffers (T 25 °C). Pigment concentration: 9.62×10^{-6} mol dm^{-3}. Al^{3+}: pigment molar ratio: 1000 : 1. The solid line is the result of the curve fitting according to eqn. (7) ($r = 0.999$).

$$AH_2 + H_2O \rightleftharpoons BH_2 + H^+ \qquad K'_h$$
$$AH_2 \rightleftharpoons AH + H^+ \qquad K_a$$
$$AH_2 + M \rightleftharpoons AM + 2H^+ \qquad K_{AM}$$
$$BH_2 + M \rightleftharpoons BM + 2H^+ \qquad K_{BM}$$
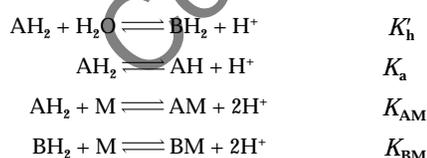
Scheme 7

expressed from the protonated ligands, the corresponding thermodynamic constants K_{AM} and K_{BM} are a_H^2 [AM]/([AH$_2$][M]) and a_H^2 [BM]/([BH$_2$][M]), M being Al^{3+} or Ga^{3+}. The values for K_{AM} and K_{BM} are reported in Table 2. From the pK_{AM} and pK_{BM} values obtained, it is clear that the affinity of Al^{3+} or Ga^{3+} for the coloured forms is much stronger than that for the colourless ones. As a consequence, at a metal–pigment molar ratio higher than 80 : 1, large concentrations of coloured forms are retained at pH 2–5. In Table 2, values for the wavelength of visible absorption maxima of the different coloured forms in their complexed forms are also reported. The strong bathochromic shifts accompanying complexation point to the pigment having, after the loss of two protons in the complex, a form similar to A. According to the data collected from molecular calculation (MM$^+$ force field, followed by semi-empirical AM1 parametrization), it appears that for the synthetic 3-deoxyflavylium chlorides, the calculated charge density in position C-3 of the flavylium–Al^{3+} or –Ga^{3+} complexes correlates with the λ_{max} of these complexes in acidic methanolic solutions. It seems that the substituent in position 3 is very important for anthocyanins to complex metals. Indeed, increasing the size and changing the nature of that substituent leads to rotation in the *B*-ring, which is certainly important in the evolution of the hydration and the complexation processes. Simulation of the electronic spectra using the CI method (AM1 parametrization) gives good results for the visible absorption maxima, showing that the calculated structures and charge density at C-3 reflect the behaviour of these pigments in solution (pigments **A3** and **A4**).

Discussion

Thermodynamic investigation in water

In slightly acidic aqueous solutions, aluminium binds moderately to a given anthocyanin requiring large aluminium : pigment molar ratios to guarantee a complete complexation. In such conditions only 1 : 1 complexes should be formed. This is no longer true in methanol due to a much stronger complexation.[10]

Al^{3+} and Ga^{3+} are small highly charged metal ions. The weak binding ability of the acetate ions (buffer) is neglected for this kind of metal but would have to be considered for some other metals, such as Mg^{2+}. The complexation equilibria are written from the completely protonated ligands AH$_2$ and BH$_2$. One should recall that BH$_2$ notation relates to the mixture of colourless forms (hemiacetal and chalcones) at equilibrium and that BM represents the corresponding mixture of aluminium complexes.

$$AH_2 \rightleftharpoons CP \qquad K_1$$
$$CP + H_2O \rightleftharpoons BH_2 + H^+ \qquad K_h^{CP}$$
$$CP \rightleftharpoons AH + H^+ \qquad K_a^{CP}$$
$$CP + M \rightleftharpoons AM^{CP} + 2H^+ \qquad K_{AM}^{CP}$$
$$BH_2 + M \rightleftharpoons BM + 2H^+ \qquad K_{BM}$$
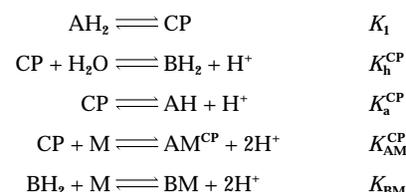
Scheme 8

At a fixed wavelength in the visible range, the absorbance may be expressed in terms of: $D = \varepsilon_{AH_2}[AH_2] + \varepsilon_{AH}[AH] + \varepsilon_A[A] + \varepsilon_{AM}[AM]$, the ε values being the molar absorption coefficients (Scheme 7). At pH lower than 5, the anionic quinonoidal base A is a very minor species and can be neglected. The total concentration of pigment can be written as: $c = [AH_2] + [AH] + [A] + [AM] + [BH_2] + [BM]$. These relations are combined with the thermodynamic constants K'_h, K_a, K_{AM}, K_{BM}

(see Results for their definitions) and K_{a2} ($K_{a2} = a_H$ [**A**]/[AH]) to give eqn. (3). Generally we can consider $K'_h \gg K_a \gg K_{a2}$,

$$D = \frac{D_0 + D_1 K_a 10^{pH} + D_2 K_a K_{a2} 10^{2pH} + D_3 K_{AM} M_t 10^{2pH}}{1 + (K'_h + K_a) 10^{pH} + K_a K_{a2} 10^{2pH} + K_{AM} M_t 10^{2pH} + K_{BM} K'_h M_t 10^{3pH}} \quad (3)$$

which leads to the more simple eqn. (4). In these equations, M_t

$$D = \frac{D_0 + D_1 K_a 10^{pH} + D_3 K_{AM} M_t 10^{2pH}}{1 + K'_h 10^{pH} + K_{AM} M_t 10^{2pH} + K_{BM} K'_h M_t 10^{3pH}} \quad (4)$$

is the total metal ion concentration and can be approximated to the free metal ion concentration because of the large metal : pigment molar ratios used in the experiments in aqueous solution. Finally, D_0, D_1, D_2 and D_3 are $\varepsilon_{AH2}c$, $\varepsilon_{AH}c$, $\varepsilon_A c$ and $\varepsilon_{AM}c$, respectively. Eqn. (4) can be checked either by varying the pH in aqueous solutions of pigment and aluminium at fixed concentrations (Fig. 1) or by varying the metal ion concentration in aqueous solutions of pigment at fixed concentration, the pH being held constant. In the first case, a curve fitting yields the best values for K_{AM} and K_{BM}, D_1 and D_3 being additional floating parameters. D_0 is determined in a solution at pH < 1, where neither hydration nor complexation take place. In the second case, for some anthocyanins, the pH is selected so that both AH and BM can be neglected. In those conditions, eqn. (3) can be rearranged in eqn. (5) (with additional simplification due to

$$\frac{1}{D} = \frac{1}{D_3} + \frac{K'_h}{D_3 K_{AM} 10^{pH}} \frac{1}{M_t} \quad (5)$$

$K'_h 10^{pH} \gg 1$) and a D vs. M_t double reciprocal plot gives a straight line from which K_{AM} can be readily estimated.

In the other cases, when AH cannot be neglected, eqn. (6)

$$D = \frac{D_1 K_a 10^{pH} + D_3 K_{AM} M_t 10^{2pH}}{1 + (K'_h + K_a) 10^{pH} + K_{AM} M_t 10^{2pH}} \quad (6)$$

gives good results, fitting correctly the experimental points (acylated anthocyanins **2**, **3**, **B**, **B1**).

For anthocyanins **2** and **3**, a special treatment is necessary, and the absorbance can be expressed at a fixed wavelength in the visible range as: $D = \varepsilon_{AH_2}[AH_2] + \varepsilon_{CP}[CP] + \varepsilon_{AH}[AH] + \varepsilon_{AM}^{CP}[AM^{CP}]$, AM^{CP} being the anthocyanin–metal complex with intramolecular complexation of the chromophore by the acyl groups (see Scheme 8). The total concentration of pigment can be expressed as: $c = [AH_2] + [AH] + [AM^{CP}] + [BH_2] + [BM] + [CP]$. The combination of these two relations with the constants K_1, K'^{CP}_h, K^{CP}_a defined before leads to eqn. (7) (Figs. 1 and 2).

$$D = \frac{D_0 + D'_0 + D_1 K^{CP}_a 10^{pH} + D_2 K^{CP}_{AM} M_t 10^{2pH}}{(1 + 1/K_1) + (K^{CP}_h + K^{CP}_a) 10^{pH} + K^{CP}_{AM} M_t 10^{2pH} + K^{CP}_{BM} K^{CP}_h M_t 10^{3pH}} \quad (7)$$

D_0, D'_0, D_1 and D_2 are $\varepsilon_{AH_2}c$, $\varepsilon_{CP}c$, $\varepsilon_{AH}c$ and $\varepsilon_{AM}^{CP}c$, respectively. At pH larger than 3, AH_2, CP, BM and BH_2 can be neglected in such a way to give eqn. (8).

$$D = \frac{D_1 K^{CP}_a 10^{pH} + D_2 K^{CP}_{AM} M_t 10^{2pH}}{(1 + 1/K_1) + K^{CP}_a 10^{pH} + K^{CP}_{AM} M_t 10^{2pH}} \quad (8)$$

The values for K'_h, K_a, K_{AM} and K_{BM} given in Tables 1 and 2 allow us to plot the relative concentrations of coloured forms as a function of pH in the presence of aluminium. Figs. 3 and 4 express the influence of the pH on metal–anthocyanin complexation and deserve a few comments.
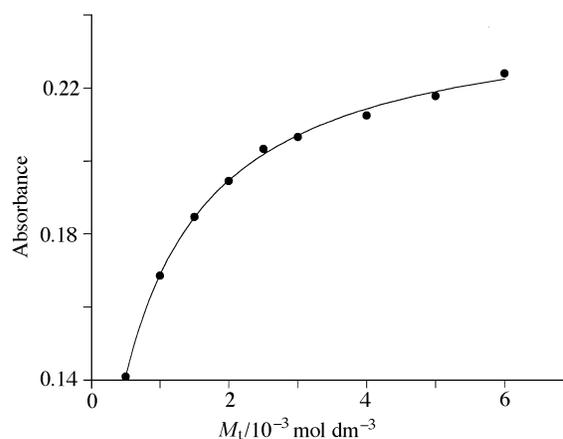
Fig. 2 Plot of absorbance (580 nm) *vs.* aluminium ion concentration of anthocyanin **3** in a 0.5 mol dm^{-3} formate buffer at pH 4.00 (*T* 25 °C). Pigment concentration: 9.62×10^{-6} mol dm^{-3}. The solid line is the result of the curve fitting according to eqn. (8) ($r = 0.999$).
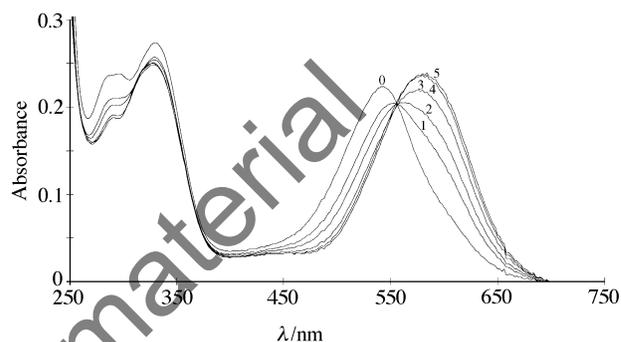
Fig. 3 UV–VIS spectra of equilibrated solutions of anthocyanin **3** in a 0.5 mol dm^{-3} formate buffer at different pH values in the presence of Al^{3+} (*T* 25 °C). Pigment concentration: 9.62×10^{-6} mol dm^{-3}. Al^{3+} : pigment molar ratio: 1000 : 1. pH = 2.42 (0); 2.74 (1); 3.00 (2); 3.51 (3); 3.80 (4); 4.16 (5).
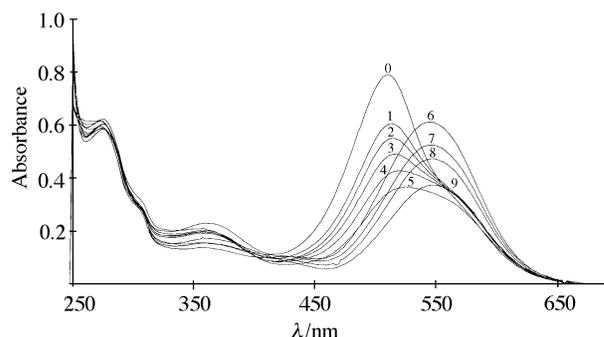

Fig. 4 UV–VIS spectra of equilibrated solutions of 3′,4′-dihydroxy-3,7-dimethoxyflavylium chloride **A2** and Al^{3+} in a 0.5 mol dm^{-3} formate buffer at different pH values (*T* 25 °C). Pigment concentration: 5.25×10^{-5} mol dm^{-3}. Al^{3+} : pigment molar ratio: 190 : 1. pH = 2.68 (0); 2.99 (1); 3.08 (2); 3.23 (3); 3.35 (4); 3.52 (5); 3.79 (6); 4.08 (7); 4.46 (8); 4.86 (9).

The first transformation taking place is hydration, regardless of whether a metal is present or not. In both cases, large amounts of colourless forms (mainly the hemiacetal) are produced and most of the colour is lost at pH 2 to 3. When the values of pK_{AM} are plotted *vs.* pK'_h (Fig. 5), it clearly appears that metal complexation is dependent on the concentration of hydrated forms except for acylated anthocyanins **1**, **2**, **3**, **B** and **B1**. In the metal containing solutions, at pH 2–3, competition between protons and metal ions for the complexing sites of the pigment are in favour of the former and no significant complexation occurs. When the pH is increased above pH 3, Al^{3+} becomes able to remove the phenolic protons of the flavylium B
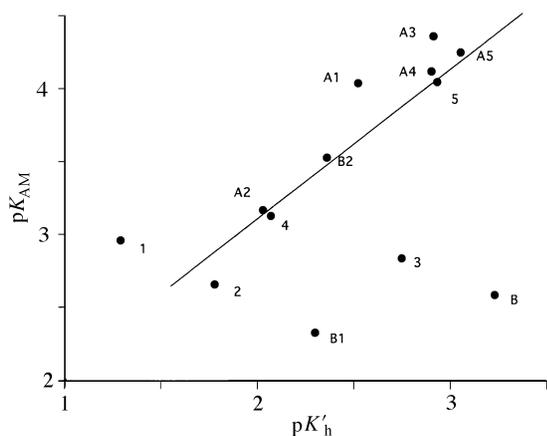
Fig. 5 pK_{AM} *vs.* pK'_h plot (in the case of aluminium complexation). The solid line indicates the correlation between hydration and metal complexation of the anthocyanins studied in this work.

Fig. 6 UV–VIS spectra of equilibrated solutions of 3′,4′-dihydroxy-7-methoxyflavylium chloride **A4** and Ga^{3+} in 0.5 mol dm^{-3} formate buffers (T 25 °C, pH = 2.59 and 4.26) followed by polychromatic irradiation for the solution at pH = 2.59. Pigment concentration: 3.22×10^{-5} mol dm^{-3}. Ga^{3+}: pigment molar ratio: 150:1. pH = 2.59 (0); pH = 2.59 (1: time of irradiation is 1 min); pH = 2.59 (2: time of irradiation is 2 min); pH = 4.26 (3); pH = 2.59 (4: subtraction of the Ga^{3+}-flavylium complex spectrum evidences the photoisomerization of the *trans*-chalcone).

ring and increasing amounts of the chelate appear as the pH is raised. This complexation process is in competition with hydration. The colour is not only strongly intensified but also very different. Indeed, in the pH domain where the flavylium ion is the dominant coloured form, complexation is accompanied by the loss of two phenolic protons so that the chromophore adopts a quinonoidal structure responsible for the deep-purple colour. From pH 4 to 5, the quinonoidal bases replace the flavylium ion; the proton activity becomes weak enough for the phenolic protons of the still abundant hemiacetal and chalcones to be replaced by aluminium and strong catechol–aluminium complexation begins to operate with those species. As a consequence, the overall hydration equilibrium is shifted towards the hemiacetal and the chalcones and the colour begins to decay (Fig. 4).

It is important to emphasize that pigment acylation selectively stabilizes the metal–anthocyanin coloured complexes through intramolecular copigmentation. In fact, the non-availability of K_{BM} values reflects the influence of these acyl groups *via* the overall conversion of the coloured forms into molecular complexes. The isosbestic point in Fig. 3 at 550 nm provides evidence for the equilibrium between the two forms CP and AM^{CP}. The presence of malonyl groups attached to a glycosyl residue seems to participate in the deprotonation of the hydroxy group at position 7 of the chromophore, leading to quinonoidal base formation at a pH lower than usually observed for most of the flavylium cations.[17] This assumption is supported by MM$^+$ molecular orbital calculations,[19] performed in a water periodic box simulating the aqueous solutions. The computed interatomic distances, for anthocyanins **2** and **3**, between the malonyl moieties and the hydroxyl at position 7 of the chromophore range from 280 to 320 pm. An interval of 300 pm is consistent with the existence of an hydrogen bond between the malonyl and the hydroxyl group of these chromophores.

Photochromism of some metalloanthocyanins

Another important aspect within the present series of pigments is the photochromic behaviour of some of our flavylium cations such as **A3** and **A4**, for instance (Fig. 6). It is now well established[20] that the colour enhancement observed upon irradiation of moderately acidic solutions of some synthetic anthocyanidins is due to a *trans*-to-*cis*-chalcone photoisomerization followed by ring closure to give the coloured flavylium cation. The same behaviour is here reported for **A3** and **A4** where irradiation of equilibrated solutions at different pH values, in the presence of Al^{3+} or Ga^{3+} leads to enhancement of the visible absorbance due to the metal-flavylium complex. The *trans*-to-*cis*-photoisomerization should thus in this particular case be immediately followed by the metalloanthocyanin ring closure.

Conclusions

Metallic complexation of anthocyanins bearing a catechol moiety is a process strong enough to induce impressive colour changes going from pale-red to deep-purple which are interpreted as a large conversion of colourless forms into a coloured chelate in which the pigment adopts a quinonoidal structure. The presence of acyl and malonyl groups seems to be fundamental for colour stabilization in weakly acidic solutions. Relative to previous reports on anthocyanin molecular interactions, this work shows the ability of not only synthetic but also natural anthocyanins to form stable complexes with small highly charged metal ions such as Al^{3+} and Ga^{3+}. Moreover, aromatic and aliphatic acylations of these pigments is demonstrated to play a role in the stability and intensity of colours exhibited by the complexes formed. This indicates a more widespread *in vivo* occurrence of supramolecular edifices constituted by acylated anthocyanins and small cations such as Fe^{3+}, Al^{3+} and/or Mg^{2+} and even other polyphenols that commonly occur in cell vacuoles.[1,2]

References

1 R. Brouillard and O. Dangles, in *The Flavonoids, Advances in Research since 1986*, ed. J. B. Harborne, Chapman and Hall, London, 1994, p. 565.
2 T. Goto and T. Kondo, *Angew. Chem., Int. Ed. Engl.*, 1991, **30**, 17.
3 R. Brouillard, G. Mazza, Z. Saad, A. M. Albrecht-Gary and A. Cheminat, *J. Am. Chem. Soc.*, 1989, **111**, 2604.
4 R. Brouillard, M. C. Wigand, O. Dangles and A. Cheminat, *J. Chem. Soc., Perkin Trans. 2*, 1991, 1235.
5 O. Dangles and R. Brouillard, *J. Chem. Soc., Perkin Trans. 2*, 1992, 247.
6 O. Dangles and R. Brouillard, *Can. J. Chem.*, 1992, **70**, 2174.
7 M. C. Wigand, O. Dangles and R. Brouillard, *Phytochemistry*, 1992, **31**, 4317.
8 K. Yoshida, T. Kondo and T. Goto, *Tetrahedron*, 1992, **48**, 4313.
9 (*a*) O. Dangles, N. Saito and R. Brouillard, *J. Am. Chem. Soc.*, 1993, **115**, 3125; (*b*) O. Dangles, N. Saito and R. Brouillard, *Phytochemistry*, 1993, **34**, 119; (*c*) P. Figueiredo, M. Elhabiri, K. Toki, N. Saito and R. Brouillard, *Phytochemistry*, 1996, **41**, 301.
10 O. Dangles, M. Elhabiri and R. Brouillard, *J. Chem. Soc., Perkin Trans. 2*, 1994, 2587.

11 N. Saito, F. Tatsuzawa, A. Nishiyama, M. Yokoi, A. Shigihara and T. Honda, *Phytochemistry*, in the press.
12 N. Toki, N. Saito, K. Kawano, T. S. Lu, A. Shigihara and T. Honda, *Phytochemistry*, 1994, **36**, 609.
13 (*a*) M. Elhabiri, P. Figueiredo, A. Fougerousse and R. Brouillard, *Tetrahedron Lett.*, 1995, **36**, 4611; (*b*) M. Elhabiri, P. Figueiredo, A. Fougerousse, O. Dangles and R. Brouillard, *Polyphénols Actualités*, 1995, **13**, 11.
14 O. Dangles and H. Elhajji, *Helv. Chim. Acta*, 1994, **77**, 1595.
15 M. Elhabiri, P. Figueiredo, F. George, A. Fougerousse, J. P. Cornard, J. C. Merlin and R. Brouillard, *Can. J. Chem.*, 1996, **74**, 697.
16 R. M. Moriaty, O. Prakash, M. P. Ducan and R. V. Vaid, *J. Org. Chem.*, 1987, **52**, 50.
17 K. R. Markham, *Techniques of Flavonoid Identification*, Academic Press, London, 1982, ch. 3.

18 P. Figueiredo, M. Elhabiri, N. Saito and R. Brouillard, *J. Am. Chem. Soc.*, 1196, **118**, 4788.
19 N. L. Allinger, *J. Am. Chem. Soc.*, 1977, **99**, 8127.
20 P. Figueiredo, J. C. Lima, H. Santos, M. C. Wigand, R. Brouillard, A. L. Maçanita and F. Pina, *J. Am. Chem. Soc.*, 1994, **116**, 1249.
21 K. Takeda, M. Koruida and H. Itoi, *Phytochemistry*, 1985, **24**, 2251.
22 K. Takeda, T. Yomashita, A. Takahashi and C. F. Timberlake, *Phytochemistry*, 1990, **29**, 1089.